

# Evaluating the influence of material selection and textile structure on liquid absorption and retention capacity in fabrics aiming for incontinence applications

*Journal of Engineered Fibers and Fabrics*

Volume 21: 1–17

© The Author(s) 2026

DOI: 10.1177/15589250261424325

[journals.sagepub.com/home/jeff](https://journals.sagepub.com/home/jeff)

Anna Björkquist<sup>1</sup> , Veronica Malm<sup>1</sup>, Behnaz Baghaei<sup>1</sup>,  
Kristian Rödbyl<sup>1</sup> and Lena Berglin<sup>1</sup> 

## Abstract

This study investigates the impact of fiber composition and fabric structure on the liquid absorption and retention performance during pressure of weft-knitted fabrics designed for reusable incontinence products. Twelve fabric samples, made from polyester, polyamide (6.6), and viscose, were knitted in two structures—1 × 1 interlock and 1 × 1 rib—with varying stitch lengths. Key parameters such as porosity, air permeability, liquid absorption capacity (LAC), and retention capacity during pressure (RCDP) were measured and analyzed. Results showed that viscose fabrics demonstrated superior LAC (up to 312%) and RCDP due to their high hydrophilicity, fiber swelling, and porosity. Polyester and polyamide had lower LAC, with polyester performing better due to higher porosity despite its hydrophobic nature. Increasing stitch length reduced fabric density and increased porosity and air permeability, thereby enhancing LAC but decreasing RCDP. Rib structures consistently exhibited higher LAC, while interlock structures offered better RCDP due to smaller, more uniform pores. The findings highlight the importance of optimizing the porous structure by altering knitting parameters and fabric structure to develop reusable absorbent textiles that balance high absorption and retention capacity during pressure.

## Keywords

liquid absorption capacity, retention capacity, weft-knitted fabric, air permeability, porosity

Received: 13 June 2025; accepted: 31 January 2026

## Introduction

Absorbent hygiene products play a vital role in managing human fluids like urine and menstrual blood. Despite the increasingly global challenge of climate change the predominant use of disposable absorbent products raises significant environmental challenges.<sup>1</sup> Data regarding waste statistics is scarce and fragmented but newly reported estimations suggest that absorbent hygiene product waste accounts for 8%–15% of total municipal waste generation.<sup>2</sup> A more specific forecast predicts that adult incontinence products alone will contribute 170 kilo tonnes of plastic waste in Australia by 2030.<sup>3</sup> Therefore the drawn

attention to circular economy and processes also involves the development of reusable alternatives which are washed and re-used many times prior to disposal. Reusable sanitary hygiene products would reduce solid waste, utilization

<sup>1</sup>Department of Textile Technology, Faculty of Textiles, Engineering and Business, University of Borås, Sweden

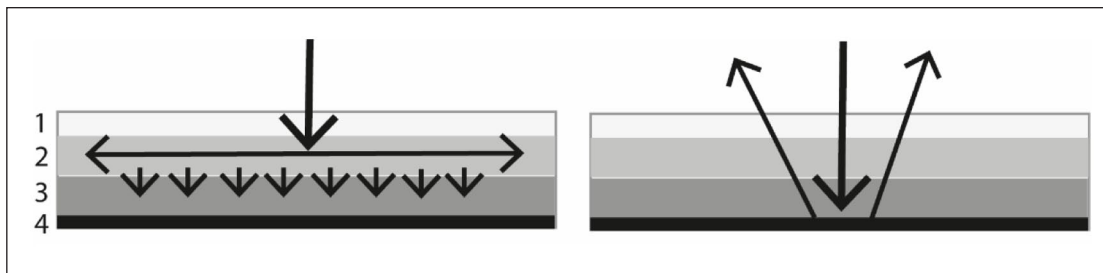
### Corresponding author:

Lena Berglin, Department of Textile Technology, Faculty of Textiles, Engineering and Business, University of Borås, Borås SE-501 90, Sweden.

Email: [lena.berglin@hb.se](mailto:lena.berglin@hb.se)



Creative Commons CC BY: This article is distributed under the terms of the Creative Commons Attribution 4.0 License (<https://creativecommons.org/licenses/by/4.0/>) which permits any use, reproduction and distribution of the work without further permission provided the original work is attributed as specified on the SAGE and Open Access pages (<https://us.sagepub.com/en-us/nam/open-access-at-sage>).



**Figure 1.** Structure and optimal versus poor flow of liquid of an absorbent incontinence product. 1: The top sheet. 2: The acquisition and distribution layer (ADL) 3: The absorbent core. 4: The leakage barrier.

of raw materials and costs for the users and health care institutions.<sup>4</sup> The transition from disposable to reusable absorbing hygiene products changes the demands of material performances, from disposable materials to materials that need to be washable and sustainable to wear and tear. Though most incontinence products are disposable there are several reusable alternatives and for many users environmental concern and economic issues are reasons to use these pads. The market for reusable menstruation items, so called period wear, has increased and several brands and products are already on the market. However, clinical studies have shown that using these products for incontinence are seen as less effective in terms of leakage and less comfortable since reusable products were found to be thick to absorb high amount liquid and the products also have a high rewet of liquid back to the surface and the human skin interface.<sup>5</sup> These issues are all a result of an ineffective liquid management in reusable textile products in terms of lower absorption and higher rewet to the surface compared to disposables.

Absorbent incontinence products are available in a range of design but generally share a common structure, typically consisting of four main layers. These layers are engineered to facilitate an optimal flow by rapid penetration, horizontal liquid distribution, absorption, and retention.<sup>6</sup> The top sheet serves as the initial point of contact, allowing urine to pass through while maintaining a dry surface in contact with the skin. Beneath this, the acquisition and distribution layer, ADL, facilitates the rapid uptake of liquid and distributes it evenly over a wide area to enhance absorption. The absorbent core is designed to capture and retain liquid, thereby keeping the upper layers dry. Finally, the back sheet acts as a waterproof barrier, preventing leakage. An optimal flow between these layers improve the retention capacity of the product, for example, the liquid is retained within the absorbent core with little or at best, no wetting back to surface. For the optimal flow of liquid both in-plane and transverse wicking are involved. Low retention capacity and high rewet back to the surface is the result of a non-optimal flow of liquid, such as poor spreading in the ADL layer and/or poor retention capacity of the absorbent core, Figure 1.

The flow of liquid through textiles involves two sequential processes, wetting and wicking. Wetting is the displacement of fiber-air interface with the fiber liquid interface and wicking is the spontaneous flow of a liquid in a porous media, driven by capillary forces caused by wetting.<sup>7,8</sup> The forces equilibrium is commonly described by Young Dupre equation (1):

$$\gamma_{SV} - \gamma_{SL} = \gamma_{LV} \cos\theta \quad (1)$$

where  $\gamma$  represents the interfacial tension that exists between the various combinations of solid, liquid and vapor, and  $\theta$  is the equilibrium contact angle. The term  $\gamma_{LV}$  is denoted as the surface tension of the liquid/vapor interface and the term  $\gamma_{LV} \cos\theta$  has been called adhesion tension or specific wettability. The contact angle may then be useful in defining the wettability of a fiber, however, the measurement of the contact angle on a rough textile structure is complicated and the equation is only valid for a drop resting on a smooth and homogenous surface. But, the magnitude of  $\cos\theta$  is useful when defining wettability. If  $\gamma_{SV}$  is larger than  $\gamma_{SL}$ , then  $\cos\theta$  must be positive, and the contact angle somewhere between  $0^\circ$  and  $90^\circ$ . Further, if  $\gamma_{SV}$  is smaller than  $\gamma_{SL}$ , then the contact angle must be between  $90^\circ$  and  $180^\circ$ . When the contact angle decreases wettability increases and when the contact angle approaches zero wettability has its maximum. The wettability of a fiber depends on the chemical nature of the fiber surface, the fiber geometry and surface roughness.<sup>9</sup> The further transport of liquid into a yarn or a fabric may then be caused by external forces or capillary forces. This means that when the liquid wets the fiber, it also reaches the spaces between fibers in the yarns (intra-yarn pores) and spaces between yarns (inter-yarn pores) in the structures and produces a capillary pressure. The magnitude of this pressure is given by the Laplace equation (2):

$$P = \frac{2\gamma_{LV} \cos\theta}{R_c} \quad (2)$$

where  $P$  is the capillary pressure in a capillary tube of Radius  $R_c$ , suggesting that the capillary pressure is higher in smaller radius. Based on fiber-liquid interactions,

further liquid transport into the yarn or fabric structure can be classified into four types: (1) capillary penetration alone; (2) capillary penetration combined with fiber imbibition, where the liquid diffuses into the fiber's interior; (3) capillary penetration along with surfactant adsorption onto the fiber surface; and (4) a combination of capillary penetration, fiber imbibition, and surfactant adsorption.<sup>7,8</sup>

For further wicking it is crucial how fast and how far the liquid may move. To model this data the Lucas Washburn equation (3) has been used:

$$L = \left( \frac{r\gamma \cos\theta_A}{2\eta} \right)^{1/2} t^{1/2} \quad (3)$$

The wicking length,  $L$ , relates to the square root of time for a structure consisting of cylindrical tubes with a constant radius,  $r$ , where these tubes are immersed in an infinite reservoir of liquid with a surface tension of  $\gamma$ , viscosity of  $\eta$ , and a constant advancing contact angle  $\theta_A$ . The equation suggests that the length increases with an increased radius, if saturation time is constant. However, there are some limitations to this model, such as the assumption of a constant advancing angle and a constant radius in yarns and fabrics. Absorbent materials, such as textiles, are porous media with structures more complex than those assumed in these equations. The pores in textiles have different sizes and are interconnected in three-dimensional networks, so that even for one-dimensional flow, the fluid must follow tortuous paths rather than a straight line as in the case of a capillary tube. Studies also show that wicking from small finite reservoirs does not follow the Lucas–Washburn model.<sup>10</sup>

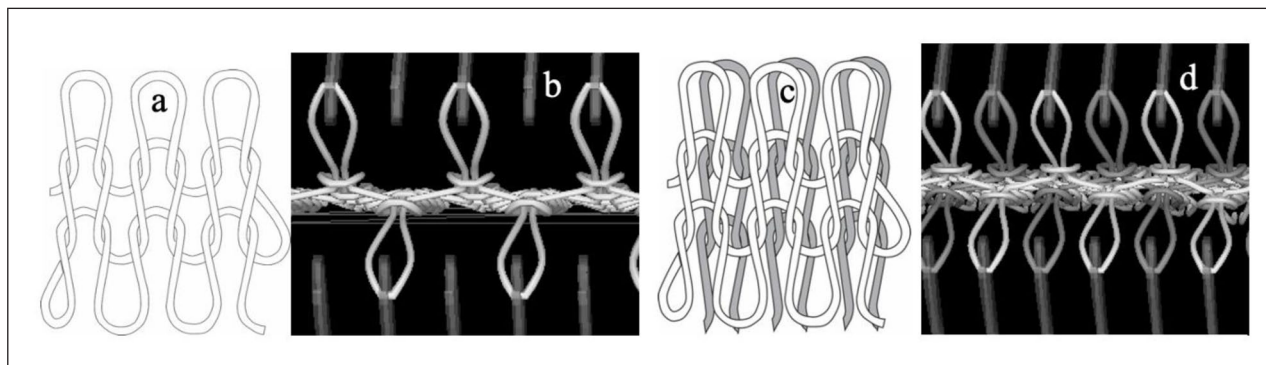
The complex processes of liquid wetting, transport (wicking) have been widely studied and both wetting and wicking in porous materials are influenced by numerous variables related to both the surface and geometric properties of the fiber, the porosity of yarn and structure, and the properties of the liquid itself.<sup>7,11</sup> Wicking is primarily driven by capillary forces, which draw the liquid through the interconnected voids in the material. This process occurs when a fabric is either fully or partially immersed in liquid or comes into contact with a small amount of liquid, such as a droplet placed on the surface.<sup>7,12,13</sup> The structure and composition of textiles play an important role in governing moisture transport. For yarns various parameters such as yarn configuration, twist, fiber shape number of fibers in yarns and surfactants influence the wicking.<sup>14–17</sup> Studies show that the wicking height for spun yarns with more evenly distributed and more packed fibers are higher. More uneven fibers distribution, hairiness and fiber covering the core slow down the wicking.<sup>14,15,18–20</sup> In fabrics both intra-yarns and inter-yarns wicking occurs which means that also fabric construction parameters influence the wicking performance.<sup>21–23</sup> In knitted textiles, the pore architecture is complex and spans multiple

scales—micro and macro. Micro pores occur within the yarn, both between individual fibers (intra-yarn pores) and between adjacent yarns (inter-yarn pores). Macro pores arise between yarns in the knitted structure, particularly in the spaces between loops and at the contact areas between yarns. Both micro and macro pores influence the overall porosity and air permeability of the material.<sup>21,24</sup> Due to this hierarchical pore structure, liquid may be found between fibers, either between filaments or yarns, in films or crevices along the fibers or inside fibers and on the surface of the fabric structure.<sup>25,26</sup> Hsieh et al. reported that wicking rates and liquid reported in a fabric depend on these pores sizes and their size distribution. According to the capillary principles the small pores are filled first and are responsible for the liquid front movement. As the smaller pores are completely filled, the liquid then moves into the larger pores.<sup>11,27,28</sup> Pores have widely varying shape and size distribution and may or may not be interconnected.<sup>13</sup> The distance of liquid advancement is greater in a smaller pore due to higher capillary pressure, but the mass of liquid retained is small. A larger amount of liquid can be retained in larger pores, but the distance of liquid advancement is limited. Fast liquid spreading in fibrous assemblies is facilitated by small uniformly interconnected pores, whereas high liquid absorption can be achieved by a larger pore. There seems to be an optimal pore size and pore size distribution for liquid spreading and retention.<sup>8,29</sup> Fischer et al. studied the wicking flow in interlacing yarns using X-ray tomographic microscopy and got a very detailed information of the intra-yarn and inter-yarn pore transition between two interlacing yarns formed as knitting two interlacing loops. As a result of these findings a wicking enhancing fabrics should include irregular pore structures, such as using profiled and mixed fiber sizes to better pore sizes between yarns.<sup>30</sup>

Liquid absorption is a specific form of wicking, where liquid is stored in the inter-yarn or intra-yarn spaces, acting as a reservoir within the textile structure.<sup>12,31,32</sup> Absorption of large volumes of liquid, such as in incontinence applications, is less frequently studied in yarn-based structures compared to pulp materials used in disposable products.<sup>33,34</sup> When evaluating the performance of disposable versus reusable incontinence products, the composition of the absorbent core is particularly critical. The absorbent core in an incontinence pad is the major component that must absorb large amounts of liquid while also retaining it under pressure. Disposable products typically incorporate advanced technologies, such as superabsorbent polymer (SAP) fibers, which are capable of absorbing and retaining substantial volumes of liquid during pressure. These materials are lightweight and maintain structural integrity even under pressure but are not intended for reuse, as their performance degrades with washing. In contrast, **reusable products** are constructed from multiple layers of yarn-based materials, designed to withstand repeated laundering while

**Table 1.** Fiber characteristics: moisture regain, density, and cross-sectional shape.

Fiber	Moisture regain % <sup>35</sup>	Crystallinity	Fiber density (g/cm <sup>3</sup> ) <sup>36</sup>	Cross-section area
Polyester	0.4	65%–85%	1.38	Round
Polyamide 6.6	4.5	65%–85%	1.14	Round
Regular viscose	12–13	35%	1.52	Irregular

**Figure 2.** 1 × 1 rib (a and b) and 1 × 1 interlock structure (c and d).

retaining their function and structure. However, due to their construction, reusable products generally exhibit lower immediate absorbency compared to disposable options. Further the integrity of reusables when it comes to leakage during press is poor, which results in higher wet back to the surface of the incontinence product.

A major challenge in the development of reusable incontinence products is therefore to achieve **high liquid absorption combined with low rewet under pressure**, enabling them to compete with the performance of disposables. While wetting, wicking, and overall liquid absorption have been widely studied in textiles, **the specific mechanisms that govern rewet and liquid retention under pressure in yarn-based absorbent structures remain largely unexplored.**

**The aim of this study is to investigate the factors influencing absorption capacity and rewet under pressure in two knitted structures composed of polyester, viscose, and polyamide.** By focusing on the interplay between fiber composition, structure, and liquid retention, this work seeks to identify key determinants of rewet performance in reusable absorbent cores. The findings are expected to provide fundamental insights for the design of next-generation reusable incontinence pads and contribute to closing the performance gap with disposable products.

## Materials and methods

### Materials

In this study, three types of smooth multifilament yarns were purchased. The fiber material of each yarn was polyester, polyamide and viscose representing three distinct

chemical compositions and moisture regain values, shown in Table 1.

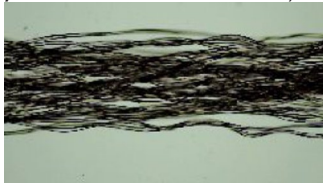
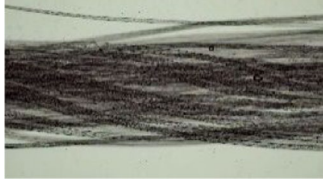
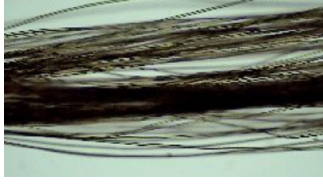
Twelve weft-knitted fabrics, characterized by differences in yarn knitting structure and stitch length, were produced using a STOLL ADF 530 ki knitting machine (7.2 gauge with 12-gauge needles) four yarns per stitch. The weft-knitted fabrics were produced in two distinct structures—1 × 1 rib and 1 × 1 interlock, Figure 2. For the interlock structure, the machine-set stitch lengths were 9.5 and 11.5, while for the 1 × 1 rib structure, the stitch lengths were set at 9 and 11. The differences in structure for the higher machine set was to get a similar loose construction. The sample material was washed five times in compliance with EN ISO 6330:2021 using machine type A, line drying, and ballast type III (100% polyester), with reference detergent 3 and a 40°C machine program 7N. The yarn specifications and fabric sample compositions are detailed in Table 2. Construction characteristics of the relaxed knits are shown in Table 3.

### Methods

**Air permeability and porosity.** The air permeability of textile fabrics was determined by measuring the rate of air flow passing perpendicularly through a specified area of fabric under a defined pressure difference across the test area within a set time period. Transverse air permeability was measured using the FX 3300 LabAir IV Air Permeability Tester, with an applied pressure of 200 Pa, in accordance with ISO 9237, 1995.

**Relative Porosity:** Porosity values were calculated using the following equation (4):

**Table 2.** Specification of the yarn and fabric samples.

Sample code	Yarn		Fabric	
	Specification	Composition	Structure	Machine setted stitch length
PES-I-1	Dtex 167/48/1 (slightly texturized yarn from Alltex/New textile) 	Polyester	1 × 1 interlock	9.5
PES-I-2		Polyester	1 × 1 interlock	11.5
PES-R-1		Polyester	1 × 1 rib	9
PES-R-2		Polyester	1 × 1 rib	11
VIS-I-1	Dtex 167/44/1 (untexturized yarn from Cofitex) 	Viscose	1 × 1 interlock	9.5
VIS-I-2		Viscose	1 × 1 interlock	11.5
VIS-R-1		Viscose	1 × 1 rib	9
VIS-R-2		Viscose	1 × 1 rib	11
POL-I-1	Dtex 156/46/1 (untexturized yarn from ContiFibre) 	Polyamide 6.6	1 × 1 interlock	9.5
POL-I-2		Polyamide 6.6	1 × 1 interlock	11.5
POL-R-1		Polyamide 6.6	1 × 1 rib	9
POL-R-2		Polyamide 6.6	1 × 1 rib	11

$$P = \left(1 - \frac{m}{\rho \cdot h}\right) \times 100 \quad (4)$$

where P is the porosity (%), m is the fabric weight ( $\text{g}/\text{m}^2$ ),  $\rho$  is the fiber density ( $\text{g}/\text{m}^3$ ), and h is the fabric thickness (m).<sup>35</sup>

**Microscopic analysis.** To investigate the pore size and interconnectivity within each sample structure, microscopic analysis was conducted using a Nikon Eclipse Ei optical microscope. This method allowed for high-resolution visualization of the internal architecture of the materials. Both dry and wet states of the samples were examined to assess the extent of fiber swelling upon hydration. The analysis specifically focused on three sample types: PES R-2, VIS R-2, and POL R-2. For each, images were captured before and after hydration to identify changes in pore geometry and fiber morphology. Pore space and fiber diameter in was measured for 5 different samples for each sample type. Comparative evaluation of the micrographs provided insights into the structural dynamics and fluid-responsive behavior of the materials.

**Analyzing absorption and retention capacity.** The specimens underwent conditioning following the SS-EN ISO 139 standard for the saturation of the moisture regain of the samples. Absorption capacity was assessed using the

drip-dry method<sup>36</sup> and measurements were conducted using ISO 20158 - Textiles—Determination of water absorption time and water absorption capacity of textile fabrics, with some modifications. Simulated urine served as the test liquid consisting of 9 g/L solution of sodium chloride in grade 3 water confirming ISO 3696, with surface tension of  $70 \pm 2 \text{ mN}/\text{m}$ . The test liquid volume was 1.5 L per test material. The textile specimen size was  $10 \times 10 \text{ cm}^2$ . The procedure involved weighing the specimen in a conditioned state, submerging a test specimen in the test liquid, and using a glass rod to force the specimen below the surface. The specimen was kept underwater for the initial 5 s and then allowed to soak freely for a total of 60 s. Afterward, the test specimen was removed from the water bath by gripping one corner with a clamp, hung up, allowed to drip for 60 s for the removal of excess liquid, and weighed to find out the liquid absorption capacity. The experiments were performed in ten replicates. The liquid absorption capacity (LAC) in % for each specimen was calculated using equation (5):

$$LAC = \frac{m_2 - m_1}{m_1} \times 100 \quad (5)$$

where  $m_1$  is the mass of test specimen in conditioned state, in g;

**Table 3.** Construction characteristics of the relaxed knitted fabrics.

Sample code	Method of measurement Mean (std)					
	SS-EN 14970:2006	SS-EN 14971:2006	SS-EN 14971:2006	-	EN ISO 5084:1999	SS-EN 12127
	Measured stitch length (mm)	Course density (cm <sup>-1</sup> )	Wale density (cm <sup>-1</sup> )	Stitch density (cm <sup>-2</sup> )	Fabric thickness (mm)	Areal density (g.m <sup>-2</sup> )
PES-I-1	5.1 (0.1)	12 (0.1)	8 (0.0)	96 (1.0)	1.80 (0.02)	631 (1.1)
PES-I-2	6.8 (0.1)	7 (0.0)	6 (0.0)	42 (0.3)	2.21 (0.1)	458 (1.7)
PES-R-1	4.7 (0.1)	13 (0.2)	7.0 (0.2)	91 (3.9)	1.80 (0.01)	570 (2.2)
PES-R-2	6.5 (0.2)	9.0 (0.3)	6.0 (0.3)	54 (1.8)	2.27 (0.03)	428 (2.9)
VIS-I-1	4.7 (0.2)	13 (0.1)	8 (0.1)	104 (2.4)	2.09 (0.03)	723 (2.3)
VIS-I-2	6.3 (0.2)	6.5 (0.3)	5.5 (0.2)	35.75 (2.5)	1.51 (0.01)	287 (3.3)
VIS-R-1	4.5 (0.2)	14 (0.5)	6 (0.2)	84 (6.0)	2.00 (0.07)	493 (3.0)
VIS-R-2	6.1 (0.2)	7 (0.2)	6 (0.2)	42 (2.7)	0.98 (0.02)	180 (2.9)
POL-I-1	5.1 (0.2)	11 (0.4)	10 (0.4)	110 (7.4)	1.66 (0.02)	775 (5.4)
POL-I-2	7.1 (0.2)	8 (0.2)	8 (0.2)	64 (3.4)	1.61 (0.02)	491 (3.0)
POL-R-1	4.8 (0.1)	13 (0.2)	13 (0.1)	169 (3.0)	1.55 (0.04)	538 (2.1)
POL-R-2	6.6 (0.1)	10 (0.1)	8 (0.1)	80 (2.3)	1.49 (0.02)	337 (1.8)

$m_2$  is the mass of test specimen in immersed state, in g.

To determine the retention capacity during pressure (RCDP), press methods used for incontinence and baby diapers were used.<sup>37,38</sup> The test procedure starts with measuring the rewet back to the surface when a specimen is subjected to pressure. Measuring involved placing a weighed dry filter paper (Munktell Quality) on top of a wet specimen, covering the specimen with a plexiglass sheet, and applying a 1 kg weight for 60 s, followed by weighing the wet filter paper. The rewet was calculated as the weight difference between filter paper after pressure and the dry filter paper. The mass of the test specimen,  $m_3$ , was calculated using equation (6).

$$m_3 = m_2 - \text{rewet} \quad (6)$$

The retention capacity was calculated (equation (7)) as ratio between retained liquid and total absorbed liquid (%)

$$RCDP = \frac{m_3 - m_1}{m_2 - m_1} \times 100 \quad (7)$$

Retention capacity during pressure refers to the capacity a textile sample holds a specific amount of liquid after pressure is applied. A high value means that the sample rewet less of the absorbed liquid to the surface during pressure. A lower value indicates higher rewet to the surface.

### Statistical analysis

Statistical analysis was conducted through an analysis of variance (ANOVA) employing a general linear model, with a significance level ( $\alpha$ ) set at 0.005 or a confidence level of 95%. Additionally, Pearson correlation and simple

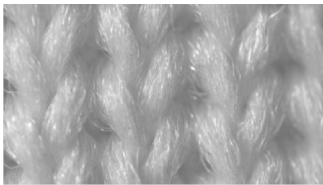
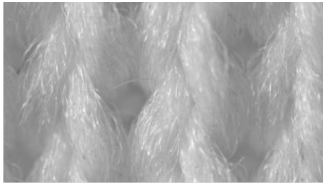

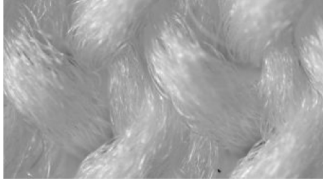




linear regression were employed to examine the relationship between thickness and air permeability.

## Results and discussion

### Fabric properties

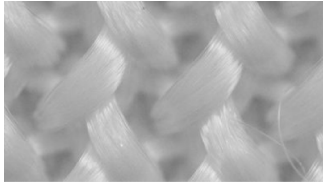



The construction parameters of knitted structures in Table 3 indicate that, even when the knitting structure (interlock or rib) and the machine-set stitch length are kept constant, changing the fiber material results in variations in actual stitch length, stitch density, and fabric thickness. For instance, in the case of polyester samples, increase in stitch length leads to a decrease in stitch density but a notable increase in fabric thickness. In contrast, viscose shows the opposite trend, where increasing stitch length does not increase thickness in the same way as polyester. For polyamide samples, the changes in stitch length and knitting structure result in minimal variations in thickness. This suggests that when comparing samples of equal surface area (e.g.  $10 \times 10 \text{ cm}^2$ ), the sample volume varies by material due to differences in thickness. It can be seen from the results shown in Table 3 that increasing the stitch length setting on the machine leads to a decrease in stitch density, fabric areal density and fabric thickness for most materials (e.g. viscose and polyamide) in both interlock and rib structures. Polyester is the main exception, as its thickness increases with stitch length, indicating a material-dependent response. Furthermore, interlock fabrics, regardless of material composition, consistently exhibit higher areal density and stitch density than rib fabrics under the same knitting conditions. The results from calculation and measurement indicate that increase of stitch length leads to increased porosity and air permeability for both interlock and rib structures as shown in Table 4.

**Table 4.** Porosity and air permeability of samples.

Sample code	Optical microscopy images	Porosity (%)	Air permeability ( $\text{l}\cdot\text{m}^{-2}\cdot\text{s}^{-1}$ )
PES-I-1		74.6	645
PES-I-2		85.0	1070
PES-R-1		77.1	651
PES-R-2		86.3	1240
VIS-I-1		76.9	462
VIS-I-2		87.3	3460
VIS-R-1		83.6	2340
VIS-R-2		87.8	6450

(continued)

**Table 4.** (continued)

Sample code	Optical microscopy images	Porosity (%)	Air permeability ( $\text{l}\cdot\text{m}^{-2}\cdot\text{s}^{-1}$ )
POL-I-1		59.0	1680
POL-I-2		73.2	5370
POL-R-1		69.6	2550
POL-R-2		80.2	5580

When comparing samples produced under the same knitting machine settings—such as PES-I-1 (74.6%), VIS-I-1 (76.9%) and POL-I-1 (59%)—the viscose samples exhibited higher textile porosity. Though the yarn density and machine setting were similar the samples exhibited different air permeability and porosity. Viscose and polyester generally exhibit higher porosity, while polyamide demonstrates the highest air permeability despite having lower overall porosity. that fiber material affects the loop configuration and pore sizes. The higher bulk and resilience of polyester yarn fill the loop decreasing both pore sizes and the air permeability.

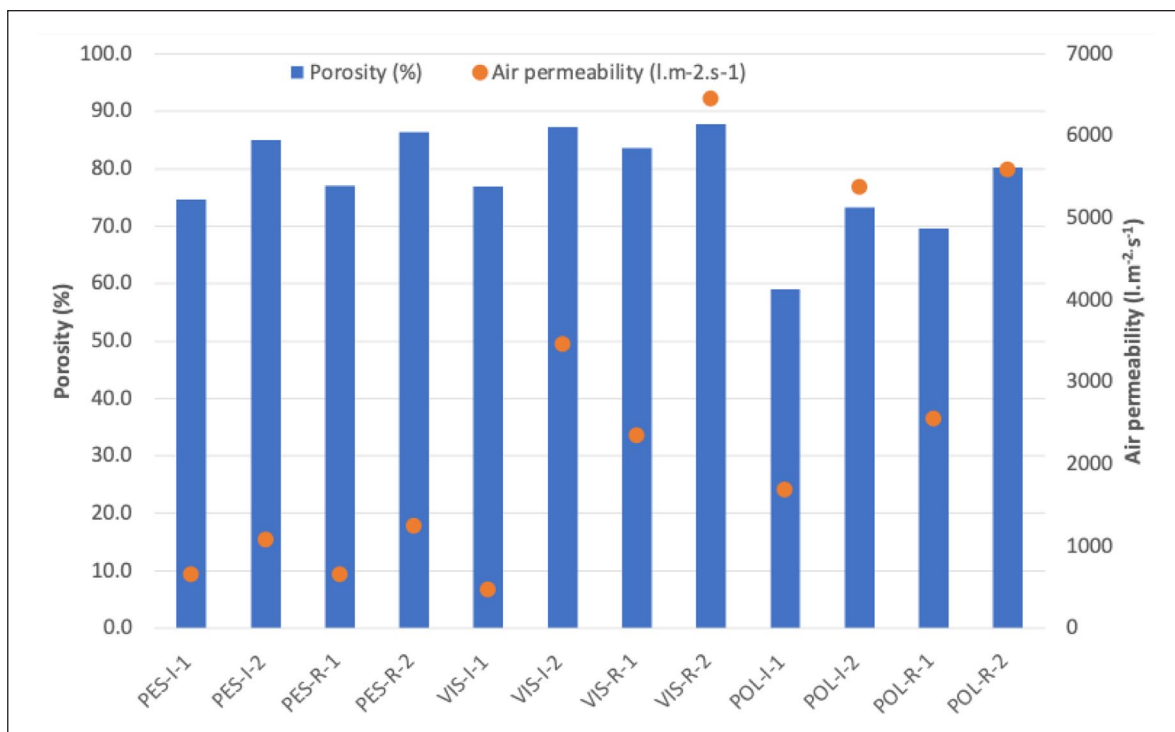
Knitting structure further influences these properties. Interlock fabrics consistently show lower air permeability compared to rib structures across all materials. Optical microscopy images (Table 4) qualitatively illustrate that interlock fabrics exhibit smaller interloop openings and a less interconnected pore morphology compared to rib structures, which tend to form larger and more open pore networks. These structural differences are consistent with the measured air permeability results, where rib fabrics allow enhanced airflow.

Yarn characteristics, particularly texturizing, also affect porosity and air permeability. Texturizing introduces crimps, loops, and increased surface roughness, which

alter fiber packing and the geometry of pore spaces. Though the yarns were categorized as smooth filament yarns the polyester yarn were slightly more texturized than the polyamide and viscose yarns. As a result, differences in airflow and porosity between fabrics cannot be attributed solely to fiber type; the texturizing process may enhance bulk and openness, especially in polyester yarns, thereby contributing to the observed lower air permeability. The viscose and polyamide yarns were denser according to the images contributing to more dense and compact loops compared to the polyester samples.

Overall, the combined effects of fiber type, knitting structure, and yarn texturizing determine the porosity and air permeability of knitted fabrics (Figure 3). Careful consideration of these factors is essential when interpreting the influence of material on fabric performance, as each parameter can significantly modify the internal pore architecture and airflow behavior.

Air permeability and porosity are two key physical properties that significantly affect liquid absorption. While air permeability is primarily influenced by porosity, it is a complex phenomenon, as air permeability and porosity can be seen as dynamic and static properties, respectively. Indeed, porosity reflects the total void space within a material, whereas air permeability indicates how



**Figure 3.** Air permeability and porosity for all samples.

open that void space is and therefore allows air (or fluid) to flow through. Samples with higher air permeability are likely to possess more continuous or aligned channels, wider connections between pores, and less tortuous flow paths. In fact, relative porosity is largely determined by the structural parameters of the fabric, such as pores and inter- and intra-yarn channels, which are in turn influenced by the bulk density.<sup>35,39</sup>

The relationship between fabric thickness and air permeability was found to be strongly material-dependent and was evaluated using Pearson correlation and simple linear regression for each material group. Figure 4 shows that polyester samples exhibited a positive correlation, where increased thickness corresponded to higher air permeability (slope  $\approx +117$ ,  $R^2 \approx 0.96$ ,  $p < 0.001$ ). This pattern reflects that greater thickness in PES results from higher stitch length and rib structures, which create looser, more open fabrics. In contrast, viscose samples showed a strong negative correlation (slope  $\approx -378$ ,  $R^2 \approx 0.94$ ,  $p < 0.001$ ), indicating that thicker VIS fabrics are substantially less permeable due to denser interlock structures and lower stitch lengths. Polyamide displayed a weak negative trend (slope  $\approx -1016$ ,  $R^2 \approx 0.18$ ,  $p = 0.061$ ), suggesting that thickness changes had minimal impact on permeability compared to other structural factors. Overall, these findings highlight that the effect of thickness on air permeability is not uniform but influenced by material type, knit structure (interlock vs rib), and stitch length, with looser

configurations generally promoting airflow and tighter, denser structures restricting it.

### Microscopic analysis of dry and wet samples

Microscopic examination of the conditioned and wet samples revealed significant swelling in the viscose fibers compared to polyester and polyamide. This swelling led to a reduction in pore size within the fabric structure. The results presented in Table 5 provide measurements for the samples, including (a) yarn diameter and (b) the size of the pores between two loops in both conditioned and wet states.

### Liquid absorption capacity (LAC%)

Liquid absorption capacity results are presented in relation to the sample porosity in Figure 5. The results show that viscose exhibits the highest LAC followed by Polyester while polyamide demonstrates the lowest absorption. The higher LAC for viscose could be explained by the lower crystallinity and hydrophilic nature of viscose enabling two types of wicking processes, liquid absorption by capillary penetration and diffusion into the amorphous regions of the fiber. Knitting structure also influences LAC %. Rib samples consistently showed higher LAC and this trend was clearer for Polyester and Viscose. Higher porosity gives higher LAC, which is clearer for PES and Viscose.

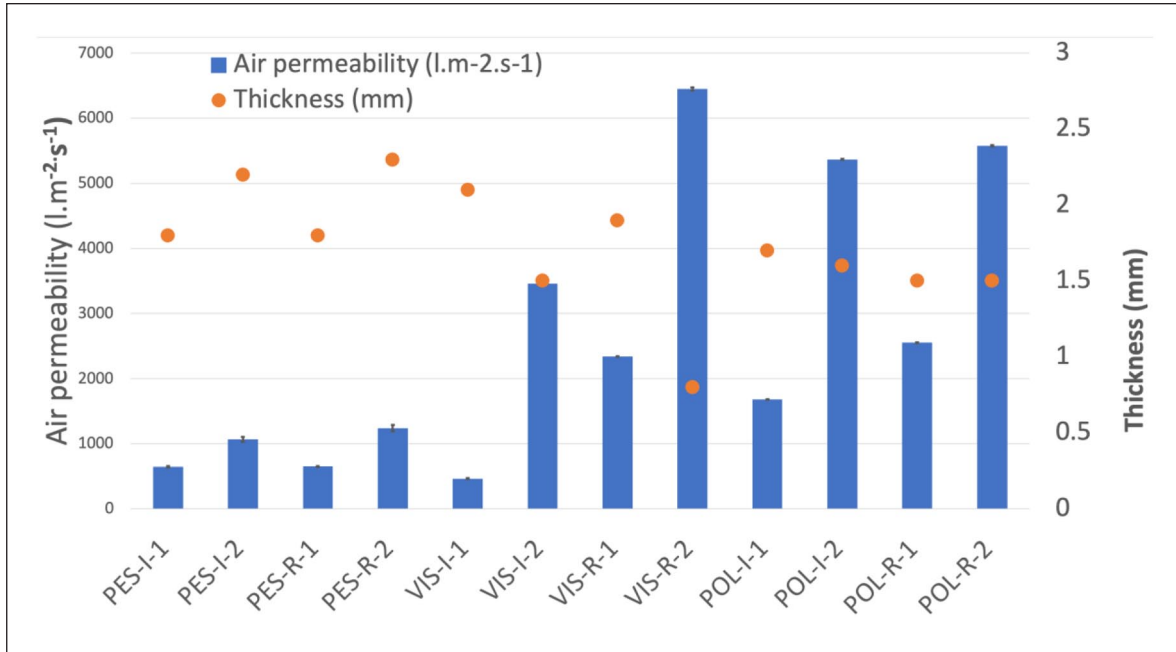
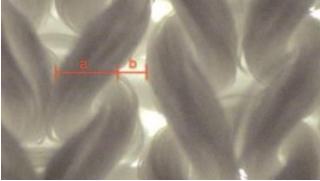
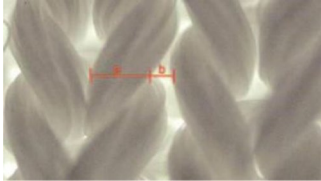
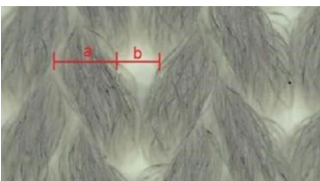
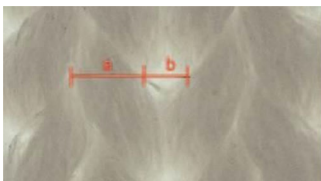
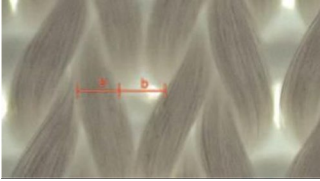
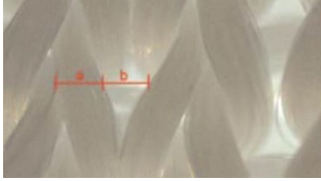
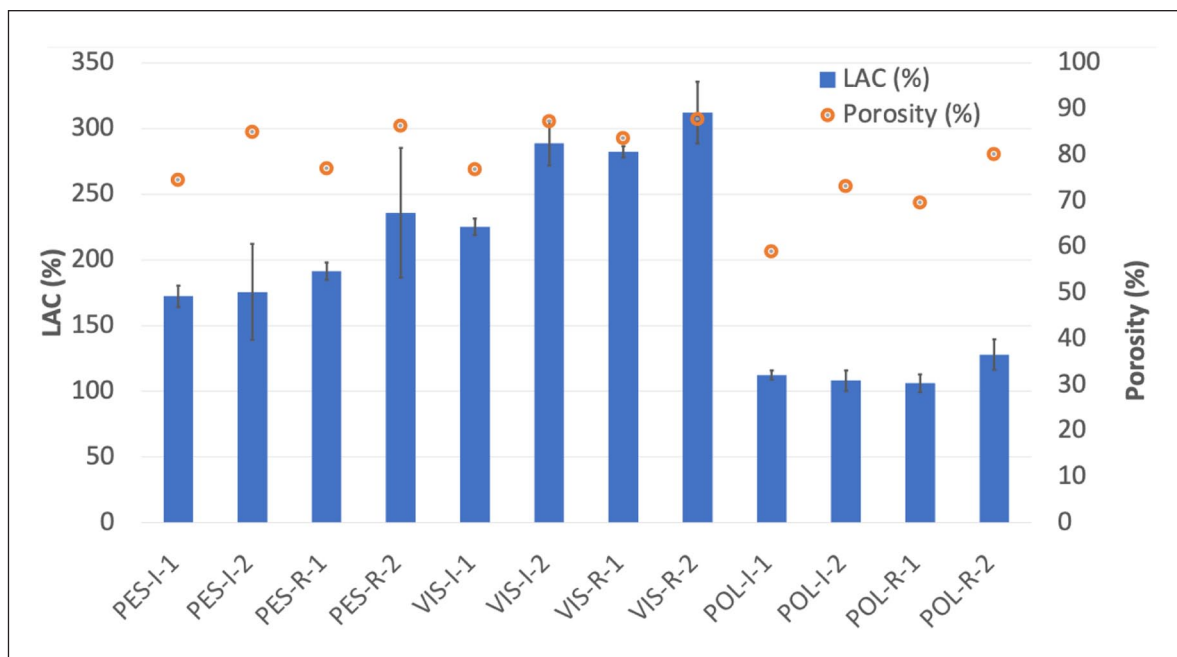


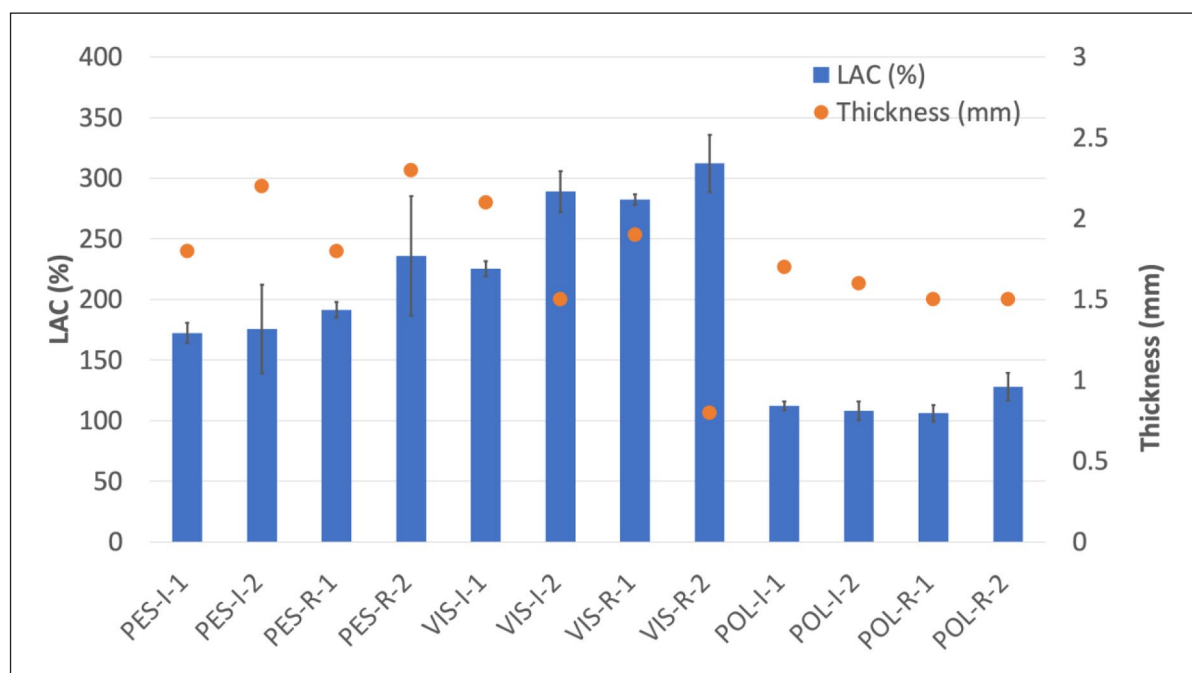
Figure 4. Air permeability and thickness for all samples.

Table 5. Yarn diameter (a) and pore size (b) measurements in dry and wet states.

Viscose dry	Viscose wet fiber (a) +23% std 1.8 Pore space (b) -29% std 1.8
	
Polyester dry	Polyester wet fiber (a) +2.3% std 0.8 Pore space (b) -4.7% std 0.9
	
Polyamide dry	Polyamide wet fiber(a) +7.9% std 6.9 Pore space (b) -6.3% std 2.8
	



**Figure 5.** Relationship between LAC and porosity for all samples.

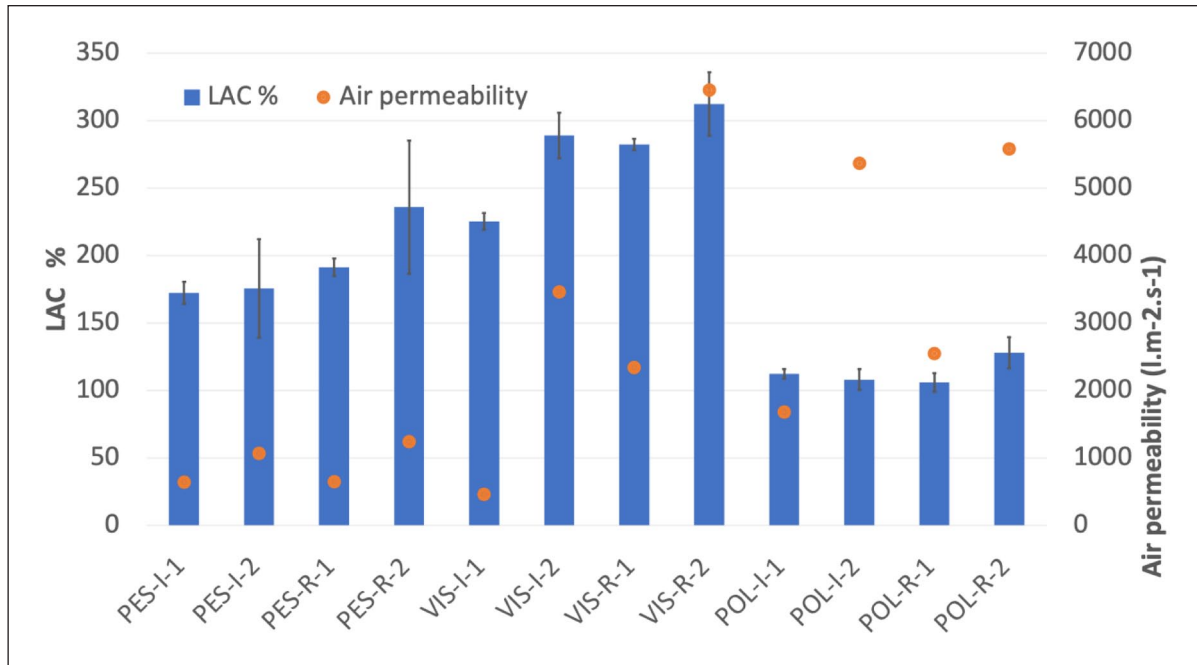


**Figure 6.** Relationship between LAC and thickness for all samples.

For Polyamide the variation of porosity results in less variation of LAC, here the absorption capacity is more in line with the slight differences of thicknesses. Another interesting aspect on thickness is that decreased sample thickness for viscose samples led to increased LAC while the opposite was shown in the polyester samples (Figure 6). This

could be related to more variation of pore sizes in the viscose samples, which should be investigated further.

The standard deviation was generally low, with an exception for PES I-2 and PES R-2. During the test polyester samples (PES-I-1 and PES-R-1) remained afloat during testing. Due to polyester's inherently hydrophobic



**Figure 7.** Relationship between LAC and air permeability for all samples.

nature, these samples were never fully immersed. Among the looser polyester structures, PES-I-2 and PES R-2, some samples were fully submerged while others were not, resulting in higher standard deviations for those samples.

Figure 7 and further illustrates the relationships between LAC, air permeability and thickness for PES, VIS, and POL samples. An increase in air permeability resulted in higher LAC values for all samples, with the exception for polyamide interlock.

The influence of stitch density knitted structure, and material type on LAC % was analyzed using statistical comparison of sample pairs, Table 6. All comparisons between different materials at both stitch densities yielded highly significant results ( $p < 0.05$ ), highlighting the dominant influence of material composition on LAC %. All material-structure pairs show significant differences. Additionally, changes in stitch density significantly affected LAC % in Viscose and Polyester rib samples, whereas no significant effect was observed in polyester interlock and polyamide interlock samples.

### Retention capacity during pressure (RCDP %)

The retention capacity during pressure is an important property of the absorbent core and the RCDP in relation to porosity is shown in Figure 8 and Table 7. The results show that the viscose samples exhibited the highest retention capacity, followed by polyamide and polyester. Porosity is in line with RCDP, but in this case a higher porosity results in lower RCDP among all samples. The

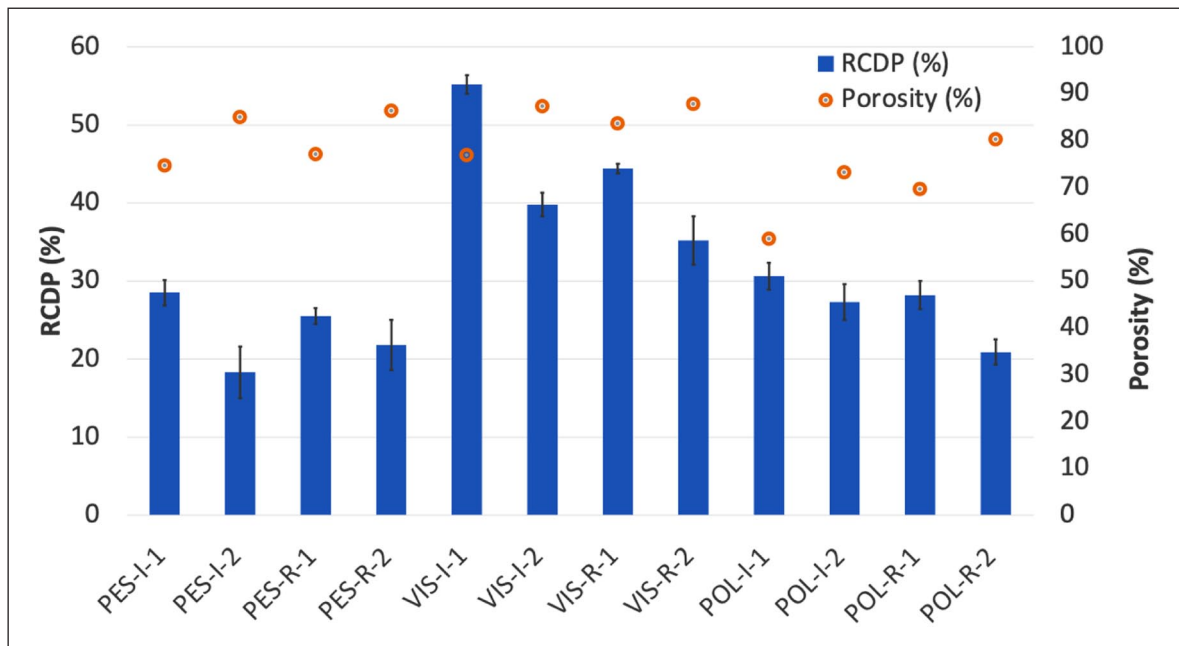
interlock samples had higher values than rib which is also the opposite from LAC. For viscose and polyamide, the higher thickness improved RCDP but for the polyester samples it was the opposite to that. The standard deviation was low for all samples except for PES-I2 and PES R-2 which is due to the higher deviations in LAC for these samples.

The relationship between RCDP, air permeability and thickness are shown in Figure 9 and Figure 10. Higher air permeability indicates a less tortuous path which led to lower retention capacity among all samples.

RCDP decreased as stitch density was reduced across all materials. Interlock samples generally showed higher RCDP (%) for all materials, likely due to their smaller interloop pore sizes. Retention is primarily governed by pore size and distribution, air permeability. Smaller pores could be better at retaining liquids due to stronger capillary forces. Narrow or bottle-necked pores prevent easy drainage, and a bimodal pore structure—containing both small and large pores—can provide a balance between absorption and retention. Fabrics with low air permeability often have more tortuous pathways that trap liquids more effectively and reduce drainage. In addition, hydrophilic fiber such as viscose attracts and retain water due to lower crystallinity and thus more amorphous areas absorbing liquid. Improving both absorption and retention. Fiber swelling could also play a role: materials like viscose swell upon contact with liquid, physically trapping liquid when larger pores decrease. Interlock samples with higher stitch densities showed higher RCDP across all materials due to their lower air permeability and porosity. This can be explained

**Table 6.** ANOVA summary table: influence of stitch density, knitted structure, and material type on LAC (%).

Comparison category	Sample pair	p-Value	Significant
Samples with two different stitch densities	PES-I-1 vs PES-I-2	0.7917	No
	PES-R-1 vs PES-R-2	0.0113	Yes
	VIS-I-1 vs VIS-I-2	$5.54 \times 10^{-10}$	Yes
	VIS-R-1 vs VIS-R-2	$9.56 \times 10^{-4}$	Yes
	POL-I-1 vs POL-I-2	0.1297	No
	POL-R-1 vs POL-R-2	$6.99 \times 10^{-5}$	Yes
Samples with different knitted structures (rib vs. interlock)	PES-I-1 vs PES-R-1	$1.65 \times 10^{-5}$	Yes
	PES-I-2 vs PES-R-2	0.0081	Yes
	VIS-I-1 vs VIS-R-1	$4.78 \times 10^{-15}$	Yes
	VIS-I-2 vs VIS-R-2	0.0128	Yes
	POL-I-1 vs POL-R-1	0.0194	Yes
	POL-I-2 vs POL-R-2	$2.73 \times 10^{-4}$	Yes
Samples with different materials	PES-I-1 vs VIS-I-1	$3.08 \times 10^{-12}$	Yes
	POL-I-1 vs VIS-I-1	$1.13 \times 10^{-20}$	Yes
	PES-I-1 vs POL-I-1	$2.72 \times 10^{-14}$	Yes
	PES-I-2 vs VIS-I-2	$5.27 \times 10^{-8}$	Yes
	POL-I-2 vs VIS-I-2	$3.21 \times 10^{-17}$	Yes
	PES-I-2 vs POL-I-2	$2.51 \times 10^{-5}$	Yes

**Figure 8.** Relationship between RCDP and porosity for all samples.

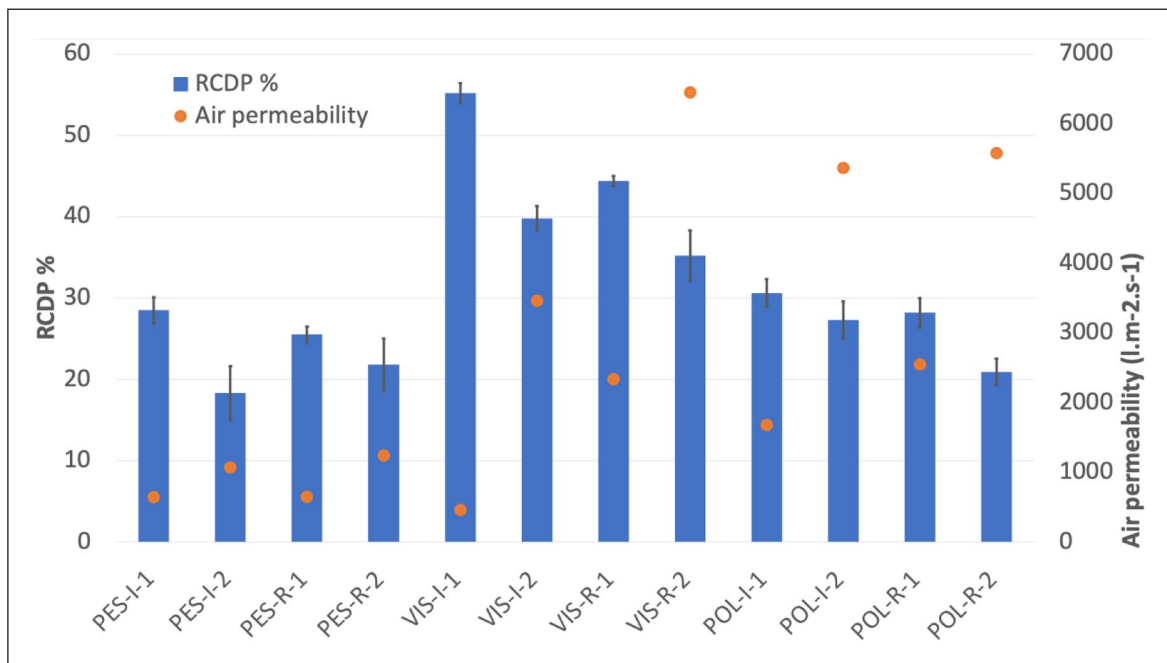
by several factors: reduced flow paths (fewer, smaller pores), higher capillary forces from smaller pores, and greater resistance to compression—all of which help retain liquid more effectively under pressure. In addition, compared to rib knits, interlock structures are more dimensionally stable because of their balanced and denser geometry. This stability prevents excessive deformation and pore collapse under pressure, thereby supporting higher liquid retention. For example, the sample VIS-I-1, which had the

lowest air permeability ( $462 \text{ l}\cdot\text{m}^{-2}\cdot\text{s}^{-1}$ ), showed the highest retention capacity.

Material composition significantly impacts liquid transport. Polyester's liquid transport relies more on textile structure than fiber absorption due to its hydrophobic and highly crystalline nature. It does not absorb water into the fiber itself but facilitates moisture movement between fibers through capillary action. In contrast, viscose is hydrophilic and amorphous, with a high

**Table 7.** ANOVA summary table: influence of stitch density, knitted structure, and material type on RCDP (%).

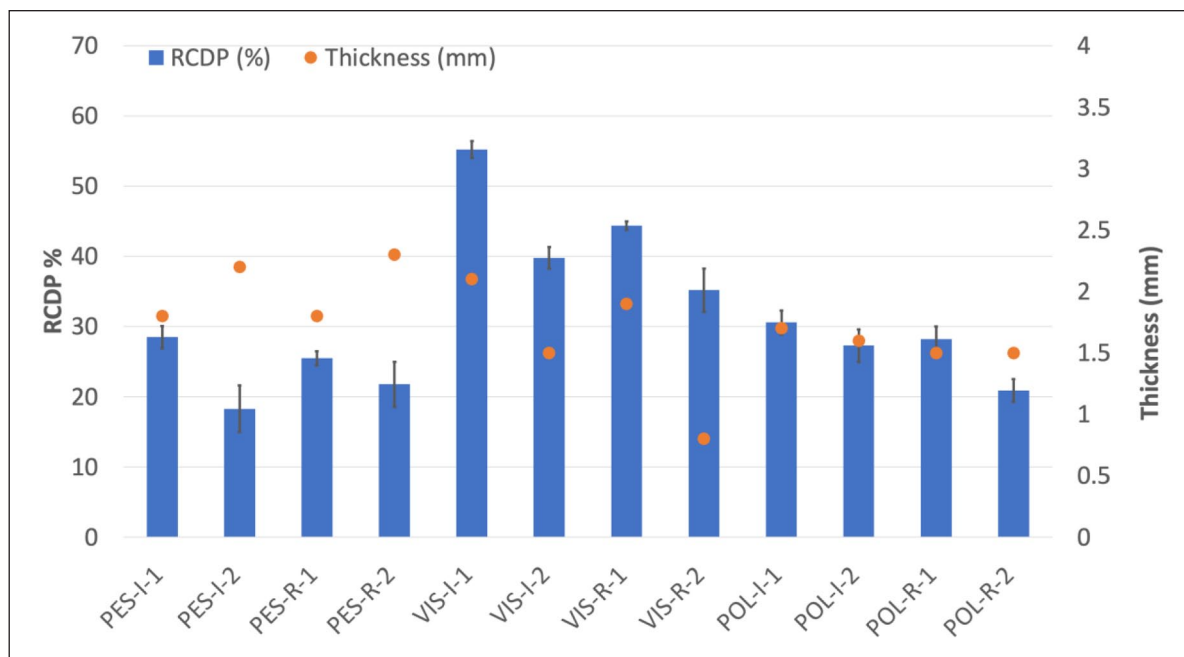
Comparison category	Sample pair	p-Value	Significant
Samples with two different stitch densities	PES-I-1 vs PES-I-2	$1.4723 \times 10^{-4}$	Yes
	PES-R-1 vs PES-R-2	$3.1388 \times 10^{-3}$	Yes
	VIS-I-1 vs VIS-I-2	$8.8199 \times 10^{-16}$	Yes
	VIS-R-1 vs VIS-R-2	$2.6926 \times 10^{-8}$	Yes
	POL-I-1 vs POL-I-2	$1.9113 \times 10^{-3}$	Yes
	POL-R-1 vs POL-R-2	$2.0102 \times 10^{-8}$	Yes
Samples with different knitted structures (rib vs interlock)	PES-I-1 vs PES-R-1	$9.4000 \times 10^{-5}$	Yes
	PES-I-2 vs PES-R-2	$2.5790 \times 10^{-1}$	No
	VIS-I-1 vs VIS-R-1	$8.6356 \times 10^{-16}$	Yes
	VIS-I-2 vs VIS-R-2	$4.2978 \times 10^{-4}$	Yes
	POL-I-1 vs POL-R-1	$6.1731 \times 10^{-3}$	Yes
	POL-I-2 vs POL-R-2	$1.0345 \times 10^{-6}$	Yes
Samples with different materials	PES-I-1 vs VIS-I-1	$1.9348 \times 10^{-19}$	Yes
	POL-I-1 vs VIS-I-1	$1.7750 \times 10^{-18}$	Yes
	PES-I-1 vs POL-I-1	$1.1907 \times 10^{-2}$	Yes
	PES-I-2 vs VIS-I-2	$1.6390 \times 10^{-7}$	Yes
	POL-I-2 vs VIS-I-2	$2.1937 \times 10^{-11}$	Yes
	PES-I-2 vs POL-I-2	$3.0609 \times 10^{-3}$	Yes

**Figure 9.** Relationship between RCDP and air permeability for all samples.

affinity for water absorption. It absorbs moisture readily, and its swelling behavior allows deeper diffusion into the fibers, resulting in faster and more complete absorption and retention.

Despite this, polyester still exhibited a higher absorption capacity than the fully immersed polyamide samples, likely due to its greater porosity. As previously discussed, porosity determines the maximum liquid-holding capacity

by defining the total void space, while air permeability affects how quickly and easily liquid can enter and flow through the material. Thus, although polyester may hold more water due to its higher porosity, its lower air permeability compared to polyamide could slow the absorption rate. It's possible that the test duration was insufficient for polyester samples to fully saturate, which explains why they did not sink during the test.



**Figure 10.** Relationship between RCDP and thickness for all samples.

## Conclusion

This study highlights the complex interaction between fiber material, knitting structure, stitch density and yarn characteristics in determining the liquid management properties of knitted fabrics. Structural parameters such as porosity, air permeability and thickness were shown to vary significantly with fiber type, even under identical machine settings and using yarns with similar yarn density. For example, Polyester fabrics exhibited increased thickness with reduced stitch density, whereas viscose fabric did not follow this trend, and the thickness of the polyamide only had slightly differences. These differences are also reflected for porosity and air permeability were a lower stitch density results in both higher porosity and air permeability for viscose and polyamide while polyester samples showed an opposite trend.

Though there are clear differences between structural parameters of the different samples the findings clearly indicate that LAC and RCDP are dictated by an interplay of fiber material, knitting structure and stitch density. Among the three fiber materials studied, viscose exhibited the highest liquid absorption capacity (LAC) and retention capacity during pressure (RCDP). This can be attributed to its highly hydrophilic nature and ability to swell and absorb liquid into the amorphous region. This dual mechanism of absorption into the structure could be a reason for viscose to effectively absorb and retain liquid during pressure. Compared to the circular fiber geometry of polyester and polyamide the irregular cross-section could also be an explanation for a more effective liquid performance, the irregular cross-section forms alternative

capillary pores between fibers within the yarns. Polyester, despite its hydrophobic and crystalline nature, still showed moderate absorption levels primarily due to higher porosity, though its retention RCDP remained the lowest. While structurally resilient and forming effective capillary pathways, highlighting the potential for surface modification of polyester to enhance hydrophilicity. Polyamide demonstrated the lowest LAC but comparatively better RCDP than polyester. The higher moisture regain of polyamide as well as polar amide groups within its chemical structure might suggest that better affinity to liquid to support a higher RCDP. Knitting structure and stitch length significantly influenced performance outcomes.  $1 \times 1$  interlock fabrics, with smaller and more uniform pores, maximized RCDP, whereas  $1 \times 1$  rib structures enhanced porosity and LAC but decreased RCDP. Similarly, longer stitch lengths reduced stitch density and areal density, resulting in higher porosity and faster absorption across all fibers, but lower RCDP. These structural differences illustrate that liquid absorption benefits from openness and porosity, while liquid retention requires restricted pore pathways and reduced deformation under pressure. Stitch density further modulated these behaviors, with higher densities generally improving retention capacity in interlock structures and influencing absorption in viscose and polyester rib knits.

Liquid absorption is influenced by both material properties and pore characteristics, including connectivity (linked to air permeability) and size (capillarity). The viscose samples, particularly those with more continuous or aligned pore structures (higher air permeability) showed

enhance the fabric's ability to absorb liquid. Pore size plays a critical role in determining the speed of liquid absorption, total absorption, smaller pores generate higher capillary pressure, which provides a stronger driving force for liquid uptake. However, viscous resistance in small pores slows the flow rate, so while they enable longer wicking distances and better liquid retention—If pores are extremely small or poorly connected, this can also limit the total absorbed volume. In contrast, larger pores exhibit lower capillary pressure, leading to faster initial flow but shorter wicking distances; they can absorb larger volumes overall but are less effective at retaining liquid.

Retention capacity during pressure has so far studied the final product performance rather than studying how RCDP is influenced by the fabric structure. Overall, optimizing fiber type, stitch length, and fabric architecture is essential to achieve a high-performance absorbent core. For the continued development of absorbent incontinence products, the key finding of this study is that structures with higher LAC tended to exhibit poorer RCDP. For example VIS-II have lower LAC than VIS-I2 but higher RCDP. Since superabsorbent fibers have extremely high LAC and RCDP at the same time, it is challenging to rely solely on the absorbent core for the development of reusable textile structures. Together with optimizing the structure of the absorbent core by altering pore sizes, fiber material and fibers sizes more focus need to be set on the ADL layer. Along with optimizing the structure of the absorbent core by altering pore sizes, fiber material, and fiber dimensions, greater focus needs to be placed on the ADL layer. Optimizing liquid distribution throughout the entire structure is a possible route for making reusable products comparable with disposables and should be further investigated. It is also clear that assessment protocols for absorbent cores and absorbent products need further development. This study has been based on standard methods commonly used in research on baby diapers and incontinence products. Although only a few results showed high standard deviations, these may have been dependent on the individual tester. Other studies have shown that the repeatability and reproducibility of these standards were poor.<sup>38</sup> For future development of incontinence products, it is also necessary to establish new methods. For example, image analysis may improve understanding, and sensors could enhance insight into the rewetting behavior of the absorbent core.

### ORCID iDs

Anna Björkquist  <https://orcid.org/0000-0001-7632-8262>

Lena Berglin  <https://orcid.org/0000-0003-0344-4128>

### Funding

The authors disclosed receipt of the following financial support for the research, authorship, and/or publication of this article:

funding from KK-stiftelsen Projekt Hög project number 20200266 and Mistra Innovation project number MI23 21.28.

### Declaration of conflicting interests

The authors declared no potential conflicts of interest with respect to the research, authorship, and/or publication of this article.

### References

1. Willskytt S and Tillman A-M. Resource efficiency of consumables – life cycle assessment of incontinence products. *Resour Conserv Recycl* 2019; 144: 13–23. <https://doi.org/10.1016/j.resconrec.2018.12.026>
2. Velasco Perez M, Sotelo Navarro PX, Vazquez Morillas A, et al. Waste management and environmental impact of absorbent hygiene products: a review. *Waste Manag Res* 2021; 39: 767–783. <https://doi.org/10.1177/0734242X20954271>
3. Thompson Brewster E, Rounsefell B, Lin F, et al. Adult incontinence products are a larger and faster growing waste issue than disposable infant nappies (diapers) in Australia. *Waste Manag* 2022; 152: 30–37. <https://doi.org/10.1016/j.wasman.2022.07.038>
4. Hait A and Powers SE. The value of reusable feminine hygiene products evaluated by comparative environmental life cycle assessment. *Resour Conserv Recycl* 2019; 150: 104422. <https://doi.org/10.1016/j.resconrec.2019.104422>
5. Fader M, Cottenden AM and Getliffe K. Absorbent products for moderate-heavy urinary and/or faecal incontinence in women and men. *Cochrane Database Syst Rev* 2008; 2008: CD007408. <https://doi.org/10.1002/14651858.CD007408>
6. Chatterjee PK. Products and technology perspective. In: *Absorbent technology*, edited by Chatterjee, P.K. and Gupta, B.S., 447–477, Elsevier Science, 2002.
7. Kissa E. Wetting and wicking. *Text Res J* 1996; 66: 660–668. <https://doi.org/10.1177/004051759606601008>
8. Patnaik A, Rengasamy RS, Kothari VK, et al. Wetting and wicking in fibrous materials. *Text Prog* 2006; 38(1): 1–105. <https://doi.org/10.1533/jotp.2006.38.1.1>
9. Miller B and Young RA. Methodology for studying the wettability of filaments. *Text Res J* 1975; 45: 359–365. <https://doi.org/10.1177/004051757504500501>
10. Kim H-S, Michielsen S and DenHartog E. Wicking in textiles at rates comparable to human sweating. *Colloids Surf A Physicochem Eng Asp* 2021; 622: 622. <https://doi.org/10.1016/j.colsurfa.2021.126726>
11. Hsieh YL, Miller A and Thompson J. Wetting, pore structure, and liquid retention of hydrolyzed polyester fabrics. *Text Res J* 1996; 66(1): 1–10. <https://doi.org/10.1177/004051759606600101>
12. Chatterjee PK and Gupta BS. Porous structure and liquid flow models. In: Chatterjee PK and Gupta BS (eds) *Absorbent technology*. Elsevier Science, 2002, pp. 1–55.
13. Hsieh Y-L. Liquid transport in fabric structures. *Text Res J* 1995; 65: 299–307. <https://doi.org/10.1177/004051759506500508>
14. Liu T, Choi KF and Li Y. Wicking in twisted yarns. *J Colloid Interface Sci* 2008; 318: 134–139. <https://doi.org/10.1016/j.jcis.2007.10.023>

15. Lu Y, Hong Q, Sun F, et al. Effect of yarn structure on the liquid moisture transport in yarns. *J Text Inst* 2022; 113: 1826–1831. <https://doi.org/10.1080/00405000.2021.1950444>
16. Nyoni AB and Brook D. Wicking mechanisms in yarns—the key to fabric wicking performance. *J Text Inst* 2006; 97: 119–128. <https://doi.org/10.1533/joti.2005.0128>
17. Öztürk MK, Nergis B and Candan C. A study of wicking properties of cotton-acrylic yarns and knitted fabrics. *Text Res J* 2011; 81: 324–328. <https://doi.org/10.1177/0040517510383611>
18. Erdumlu N and Saricam C. Wicking and drying properties of conventional ring- and vortex-spun cotton yarns and fabrics. *J Text Inst* 2013; 104: 1284–1291. <https://doi.org/10.1080/00405000.2013.799258>
19. Li Q, Wang JJ and Hurren CJ. A study on wicking in natural staple yarns. *J Nat Fibers* 2017; 14: 400–409. <https://doi.org/10.1080/15440478.2016.1212763>
20. Perwuelz A, Mondon P and Caze C. Experimental study of capillary flow in yarns. *Text Res J* 2000; 70: 333–339.
21. Birrfelder P, Dorrestijn M, Roth C, et al. Effect of fiber count and knit structure on intra- and inter-yarn transport of liquid water. *Text Res J* 2013; 83: 1477–1488. <https://doi.org/10.1177/0040517512460296>
22. Datta Roy M, Chattopadhyay R and Sinha SK. Wicking performance of profiled fibre part B: assessment of fabric. *J Inst Eng (India) Ser E* 2018; 99: 1–8. <https://doi.org/10.1007/s40034-017-0103-2>
23. Parada M, Derome D, Rossi RM, et al. A review on advanced imaging technologies for the quantification of wicking in textiles. *Text Res J* 2017; 87: 110–132. <https://doi.org/10.1177/0040517515622151>
24. Hettiarachchi D, Michielsen S, Wen C, et al. Liquid moisture wicking in textile and inter-fibre pore filling behaviour in yarns: a review. *J Text Inst* 2025; 116: 2500–2519. <https://doi.org/10.1080/00405000.2024.2440062>
25. Bentoufa S, Fayala F and BenNasrallah S. Capillary rise in macro and micro pores of jersey knitting structure. *J Eng Fibers Fabr* 2008; 3: 47–54.
26. Duprat C. Moisture in textiles. *Annu Rev Fluid Mech* 2022; 54: 443–467. <https://doi.org/10.1146/annurev-fluid-030121-034728>
27. Kim H-S, Michielsen S and DenHartog E. New wicking measurement system to mimic human sweating phenomena with continuous microfluidic flow. *J Mater Sci* 2020; 55: 7816–7832. <https://doi.org/10.1007/s10853-020-04543-4>
28. Hsieh YL, Thompson J and Miller A. Water wetting and retention of cotton assemblies as affected by alkaline and bleaching treatments. *Text Res J* 1996; 66: 456–464.
29. Chattopadhyay R. Wicking behavior of compact and ring spun yarns and fabrics. One day seminar on Comfort in Textile, Dept of Textile Technology IIT Delhi, New Delhi, 16 October 2004, p. 16.
30. Fischer R, Schlepütz CM, Rossi RM, et al. Wicking through complex interfaces at interlacing yarns. *J Colloid Interface Sci* 2022; 626: 416–425. <https://doi.org/10.1016/j.jcis.2022.06.103>
31. Fischer R, Schlepütz CM, Zhao J, et al. Wicking dynamics in yarns. *J Colloid Interface Sci* 2022; 625: 1–11. <https://doi.org/10.1016/j.jcis.2022.04.060>
32. Mhetre S and Parachuru R. The effect of fabric structure and yarn-to-yarn liquid migration on liquid transport in fabrics. *J Text Inst* 2010; 101: 621–626. <https://doi.org/10.1080/00405000802696469>
33. Gupta BS. Fluid absorption in high bulk nonwovens. In: Chatterjee PK and Gupta BS (eds) *Absorbent technology*, Elsevier Science, 2002, pp.93–127.
34. Hollies N, Kaessinger MM and B W. Water transport mechanism in textile materials. Part II. Capillary-type penetration in yarns and fabrics. *Text Res J* 1957; 27: 8–13.
35. Bedek G, Salaün F, Martinkovska Z, et al. Evaluation of thermal and moisture management properties on knitted fabrics and comparison with a physiological model in warm conditions. *Appl Ergon* 2011; 42: 792–800. <https://doi.org/10.1016/j.apergo.2011.01.001>
36. Gupta BS and Chatterjee PK. Measurement techniques for absorbent materials and products. In: Chatterjee PK and Gupta BS (eds), *Absorbent technology*, Elsevier Science, 2002, pp.389–446.
37. Cottenden AM, Dean GE and Brooks RJ. Predicting the leakage performance of small bodyworn disposable incontinence pads using laboratory tests. *Med Eng Phys* 1997; 19: 556–571.
38. Cottenden AM, Rothwell JG, Leander H, et al. A critical investigation of ISO 11948-2 and ISO 11948-1 for predicting the leakage performance of small disposable incontinence pads for lightly incontinent women. *Med Eng Phys* 2006; 28: 42–48. <https://doi.org/10.1016/j.medengphy.2005.03.006>
39. Gidik H, Vololonirina O, Ghantous RM, et al. Impact of test parameters on the water vapor permeability of textiles. *Int J Clothing Sci Technol* 2019; 31: 350–361. <https://doi.org/10.1108/IJCST-02-2018-0018>